A&A 484, 703–709 (2008)
DOI: 10.1051/0004-6361:20079100

Astronomy & Astrophysics

The Hα Galaxy survey*

V. The star formation history of late-type galaxies

P. A. James, M. Prescott, and I. K. Baldry

Astrophysics Research Institute, Liverpool John Moores University, Twelve Quays House, Egerton Wharf, Birkenhead CH41 1LD, UK
e-mail: paj@astro.livjm.ac.uk

Received 19 November 2007 / Accepted 7 April 2008

ABSTRACT

Aims. This study of 117 low-redshift Im and Sm galaxies investigates the star formation rates of late-type galaxies, to determine whether they are quasi-continuous or dominated by bursts with quiescent interludes.
Methods. We analyse the distribution of star formation timescales (stellar masses/star formation rates) for the entire sample, and of gas depletion timescales for those galaxies with gas mass measurements.
Results. We find that, on average, the late-type galaxies studied could have produced their total stellar masses by an extrapolation of their current star formation activity over a period of just under a Hubble time. This is not the case for a comparison sample of earlier-type galaxies, even those with disk-dominated morphologies and similar total stellar masses to the late-type galaxies. The earlier-type galaxies are on average forming their stars more slowly at present than the average rate over their past histories. No totally quiescent Im or Sm galaxies are found, and although some evidence of intrinsic variation in the star formation rate with time is found, this is typically less than a factor of 2 increase or decrease relative to the mean level. The Im and Sm galaxies have extensive gas reservoirs and can maintain star formation at the current rate for more than another Hubble time. The average spatial distribution of star formation in the Im galaxies, and to a lesser extent the Sm galaxies, is very similar to that of the older stellar population traced by the red light.
Conclusions. Late type, bulge-free galaxies have a predominantly continuous mode of star formation, and could have assembled their stellar masses through continued star formation over a Hubble time with the currently-observed rate and spatial distribution. There is little evidence in this sample of predominantly isolated field galaxies of significant star formation through brief but intense starburst phases.

Key words. galaxies: general – galaxies: spiral – galaxies: irregular – galaxies: fundamental parameters – galaxies: stellar content

1. Introduction

Late-type galaxies of type Im and Sm are pure "blue sequence" star forming systems, with little or no old bulge component, and are the most numerous low-luminosity galaxy type in the field environment. The star formation (SF) histories of these galaxies are of interest for several reasons. Low luminosity galaxies typically have shallow potential wells, and are thus more susceptible to the effects of internal feedback from stellar winds and supernovae (Dekel & Silk 1986; Dekel & Woo 2003; Stinson et al. 2006). They are also likely to be affected by external factors such as the intergalactic ultraviolet radiation field (Somerville 2002; Grebel & Gallagher 2004) which can suppress SF in the lowest mass galaxies. There is also significant current interest in the fate of dwarf galaxies falling into galaxy groups or clusters from the field environment (Mayer et al. 2001); disentangling the effects of environment on such galaxies requires a good knowledge of the range of SF activity exhibited by isolated systems. In order to address such statistical questions, large numbers of galaxies should be investigated. This is particularly true for the lowest luminosity systems, for which SF indicators such as Hα flux (used in the present paper) may be substantially affected by statistical fluctuations (Weilbacher & Fritze-v. Alvensleben 2001).

The present study looks at SF activity of 42 Sm and 75 Im galaxies from the Hα Galaxy Survey (HαGS; James et al. 2004). The analysis centres on the SF timescale for each of the galaxies studied, where this timescale is defined as the ratio of the total stellar mass to the current SF rate. This method is thus closely related to the stellar birthrate parameter pioneered by Kennicutt et al. (1994). The distribution of SF timescales provides a test of whether SF is continuous, as found observationally by e.g. Gallagher et al. (1984) and van Zee (2001), or in temporally separated bursts. The latter have been predicted by theoretical studies such as the Stochastic Self-Propagating Star Formation models of Gerola et al. (1980), and by recent simulations carried out by Stinson et al. (2007). Observational evidence of burst-dominated SF in dwarfs has been found by Almoznino & Brosch (1998) in a study of late-type Virgo cluster dwarfs, and by Barazza et al. (2006) who looked at dwarf galaxies over to redshift range 0.02–0.25. In addition, studies based on abundance ratios and comparison with chemical evolution models have found evidence of burst-dominated SF histories in Local Group dwarfs, and in blue compact galaxies (Lanfranchi & Matteucci 2003; Recchi et al. 2006).

The present study is the largest sample of local late-type galaxies studied using Hα imaging. The 117 galaxies of the

* Based on observations made with the Jacobus Kapteyn Telescope operated on the island of La Palma by the Isaac Newton Group in the Spanish Observatorio del Roque de los Muchachos of the Instituto de Astrofísica de Canarias.

present sample constitute ~55% of the known Sm and Im galaxies satisfying the selection criteria of the HαGS sample, and they are all of the observed galaxies of these types in the HαGS study. Thus we can with confidence extrapolate any results found to the general population of late-type field galaxies in the local Universe; there is no reason to suspect any systematic differences between the 55% of galaxies observed and the remaining 45%.

We also carry out further tests of SF activity in HαGS galaxies, using subsets of objects for which other data are available. The 2MASS database (Jarrett et al. 2003) provides homogeneous near-infrared (NIR) photometry for 201 out of the full sample of 334 HαGS galaxies, over all morphological types. We calculate our own J and K total magnitudes for these galaxies, based on the 2MASS aperture photometry, and hence derive stellar mass estimates as a check on those derived from our own R-band photometry. The $R-K$ and $J-K$ total colours can also be compared with the predictions of stellar population synthesis models, giving a consistency check on our conclusions about the SF activity in the late-type galaxies and the mass-to-light (M/L) ratios assumed in the calculation of the SF timescales.

Gas masses derived from HI observations are available for 94 galaxies in the HαGS sample from the Westerbork observations of neutral Hydrogen in Irregular and SPiral galaxies (WHISP) survey (Swaters et al. 2002). This enables a calculation of the gas depletion times for galaxies of different types, which gives a further consistency check on our conclusions.

Finally, we compare the spatial distributions of forming and old stellar populations in the late-type galaxies, from the Hα and R-band imaging respectively, to test whether the overall structures of galaxies are consistent with their having been built up by SF activity distributed like that seen currently.

The structure of the current paper is as follows. Section 2 contains a description of the galaxy sample, the data used and the calculation of stellar masses for all galaxies. Section 3 outlines the calculation of the timescale required for the formation of the total stellar mass of each galaxy, given the current SF rate derived from Hα emission. Section 4 similarly looks at the timescale for the conversion of the current gas reservoirs into stars, assuming continued SF at the current rate. These conclusions are combined in Sect. 5 in an analysis of the "burstiness" of SF, i.e. the extent to which the SF rate of individual galaxies varies about the mean level. Section 6 contains an analysis of the extent to which the conclusions depend on specific stellar population synthesis models used, and whether the initial assumptions used to calculate the stellar M/L ratio are consistent with the final conclusions. Section 7 is a summary of the main conclusions.

2. Photometric data and derived quantities

The Hα Galaxy Survey (HαGS) is a study of the SF properties of galaxies in the local Universe, using fluxes in the Hα line to determine the total rates and distributions of SF within the selected galaxies. The observations cover 334 galaxies, all of which were observed with the 1.0 m Jacobus Kapteyn Telescope (*JKT*), part of the Isaac Newton Group of Telescopes (ING) situated on La Palma in the Canary Islands. The selection and the observation of the sample are discussed in James et al. (2004), hereafter Paper I, but to summarise, galaxies were selected from the Uppsala General Catalogue of Galaxies (Nilson 1973) with diameters between 1.′7 and 6.′0, recession velocities less than 3000 km s^{-1}, and Hubble types from S0a – Im inclusive. The Virgo cluster region was excluded from selection, so this is predominantly a field galaxy sample. Approximately 50% of the galaxies (and almost all of the Sm and Im types) are within a 15 Mpc radius from the Milky Way but, given the diameter upper limit, no Local Group objects are included. Thus the late-type (Sm and Im) sample closely resembles that of van Zee (2001) in terms of environment, distance and luminosity, but differs from samples studied via analysis of resolved stellar populations, where the galaxies tend to be nearby low-surface-brightness extreme dwarfs. All HαGS R-band magnitudes and Hα fluxes used here are corrected for Galactic extinction according to the methods of Schlegel et al. (1998).

Table 1. Mean colours and M/L ratios in the R and K bands as a function of galaxy T-type.

Galaxy T-type	$(B-R)$	$(M/L)_R$	$(M/L)_K$
0–2	1.50	2.86	0.80
3–4	1.30	1.93	0.65
5–6	1.25	1.75	0.62
7–9	1.00	1.07	0.47
10	0.74	0.65	0.36

2.1. Stellar masses

Stellar masses were initially derived from the R-band total magnitudes of each of the HαGS galaxies, with the M/L ratio being derived from the models of Bell & de Jong (2001) and a type-dependent $(B-R)$ colour taken from Bell & de Jong (2000). Table 1 lists the mean adopted colours and the resulting M/L ratios as a function of galaxy type. Bell & de Jong (2001) base their models on a Salpeter IMF but scale it by a factor 0.7 to avoid violating dynamical disk mass limits ("diet Salpeter"). This also brings the M/L ratios closer to the Chabrier (2003) and Kroupa (2001) IMFs which contain fewer low-mass stars than implied by a single power law.

Errors on the R-band-derived stellar masses result from photometric errors (typically 10% for our R-band photometry), internal extinction errors (taken as 50% of the Hα extinction errors, explained in Sect. 2.2 below) and uncertainties in the M/L ratios from modelling, which we took as 40%. These stellar masses thus have errors in the range 43–48%, with the larger values corresponding to the brighter galaxies.

A check on the stellar masses of many galaxies was provided by the availability of 2MASS NIR photometry for 201 galaxies in the HαGS sample. The NIR has significant advantages over the optical in this context; extinction corrections are much smaller, and in general M/L variations are a weaker function of SF history, in the redder passbands. However, there are limitations of the 2MASS database for the current study, as many of the latest-type galaxies have low surface brightnesses in the NIR and are not detected by 2MASS. Care was needed in allocating total J and K magnitudes to those galaxies that were in the 2MASS database. In many cases, the published 2MASS extrapolated magnitudes, $J_{\rm ext}$ and $K_{\rm ext}$, were found to be too faint by several tenths of a magnitude, e.g. by comparison with 2MASS circular aperture photometry. This is due to a known problem with the 2MASS extrapolation algorithm, which can lose flux for extended objects of low surface brightness (Jarrett, private communication). For all affected galaxies, we derived our own $J_{\rm tot}$ and $K_{\rm tot}$ magnitudes, by matching 2MASS circular aperture photometry to our own R-band growth curve, which was derived from matched circular apertures, and assuming an identical Δm

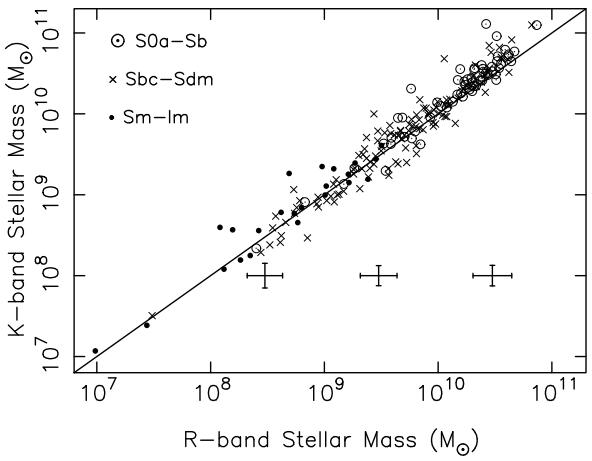

Fig. 1. The K-band derived stellar mass versus the R-band derived stellar mass for the 201 galaxies with 2MASS photometry. Three representative error bars are shown, corresponding to galaxies with masses $<10^9$ $M_\odot$; 10^9 $M_\odot$ – 10^{10} $M_\odot$; and $>10^{10}$ $M_\odot$, respectively.

between the largest aperture and the asymptotic total magnitude in the R, J and K passbands. This assumes the $R-J$ and $R-K$ colour gradients are small in the outer regions of these galaxies.

After applying these methods, we have homogeneous $J_{\rm tot}$ and $K_{\rm tot}$ magnitudes for 201 of the HαGS galaxies, more than 50% of the total, although this is biased towards the brightest and highest surface brightness types. In particular, only 8 Sm and 13 Im galaxies have total 2MASS magnitudes, and these are very much weighted towards the brightest examples of these types.

Figure 1 provides a check on the reliability of the R-band stellar mass estimates, using the 2MASS $K_{\rm tot}$ magnitudes described above. The quantities plotted on the vertical and horizontal axes are the individual galaxy stellar masses estimated from the K- and R-band magnitudes respectively, using M/L ratios from Bell & de Jong (2001) as in Table 1. Stellar masses derived from K-band photometry are subject to the same sources of error as those from R-band photometry. Although the formal errors on the published 2MASS data are small, the total magnitudes used here have significant uncertainties due to the extrapolation procedure described above. This gives the largest errors (0.3 mag) for the faint galaxies, falling to 0.2 mag for the brightest ones. Extinction and M/L modelling uncertainties are smaller than for the R-band, ~25%. Thus the total errors in K-band-derived stellar masses are 42% for the lower-luminosity galaxies, falling to 33% for the bright spirals.

Figure 1 shows a significant scatter in the mass estimates from the two passbands, with individual galaxies showing discrepancies as large as a factor of 3, in either sense. The typical error bars shown in Fig. 1 are calculated from the error sources described above, and do not include contributions due to galaxy distance uncertainties, since these affect both mass estimates equally and do not contribute to the scatter.

It can be noted from Fig. 1 that there is a small but systematic offset in the sense that the K-band-derived masses are slightly larger than those from the R-band luminosity. This offset is a factor of 1.12 ± 0.08 in the mean for galaxies with masses below 10^9 $M_\odot$; 1.09 ± 0.04 for galaxies between 10^9 and 10^{10} $M_\odot$; and 1.28 ± 0.04 for galaxies more massive than 10^{10} $M_\odot$. This may indicate a systematic offset inherent in the M/L modelling, or under-correction for internal extinction which would preferentially affect the brighter galaxies. In any case, the effect is small compared with other sources of error for the faint Sm and Im galaxies with which the present paper is primarily concerned. The R-band stellar masses were used in the rest of our analysis, since these are available for the full sample of galaxies.

2.2. Star formation rates

The SF rates quoted in James et al. (2004) were determined from the Hα fluxes using the Kennicutt (1998) conversion factor for a Salpeter (1955) stellar initial mass function (IMF) from 0.1 to 100 $M_\odot$. However, as explained above, several studies have now concluded that this IMF results in an unrealistically high total stellar mass, and one solution is to multiply all stellar masses and SF rates by 0.7. Since this is done for the stellar mass estimates used here, for consistency we scale the SF rates from James et al. (2004) by the same factor of 0.7. We assume that the IMF is universally applicable. If the IMF varies between galaxies, as suggested by Hoversten & Glazebrook (2007), there could be substantial variations in the conversion of Hα flux to SF rate and colour to stellar mass that will affect the timescale determinations.

There are several contributors to the errors on derived SF rates. The Hα fluxes have errors which are dominated by uncertainties in continuum subtraction (James et al. 2004), with further contributions due to filter throughput, sky background and photometric calibration uncertainties. In total, the Hα flux errors for the lower luminosity galaxies in which we are most interested here are of order 25%, falling to 10% for the brighter galaxies with strong Hα emission. The other major sources of error in the calculated SF rates arise from the adopted extinction corrections, and to a lesser extent the corrections for the [NII] lines that lie in the bandpass of the narrow band filters used. Several sets of such corrections were investigated, including those of Kennicutt (1983), a type-dependent correction from James et al. (2005), and corrections dependent on R-band total magnitudes, following the prescription of Helmboldt et al. (2004). The latter were adopted for the present paper, and following an intercomparison of the size of the extinction corrections from the different methods, errors were assigned of 0.4 mag. for the brightest spiral galaxies, falling to 0.26 mag for the fainter spirals and 0.16 mag for the faintest galaxies, including almost all of the Sm and Im types. This error corresponds to about 50% of the size of the applied extinction correction. Combining the Hα flux and extinction errors, the overall errors on SF rates are 30% for the faintest galaxies, rising to 50% for the brightest spirals, with the rise being due to the larger, and hence more uncertain, extinction corrections for larger galaxies.

3. Analysis of star formation timescales

The initial analysis involved the calculation of the time required to form the total stellar mass of each galaxy studied, under the assumption of continuous SF at the current rate. This was given by

$$\text{SF timescale} = \frac{\text{stellar mass}}{\text{SFR}} \frac{1}{(1-\mathcal{R})} \quad (1)$$

where $\mathcal{R}$ is the mass recycled to the interstellar medium per mass of stars formed. The factor $\mathcal{R}$ is taken to be 0.4 as per van Zee (2001). The metallicity dependence of $\mathcal{R}$ was investigated using the BaSTI population synthesis model (Pietrinferni et al. 2004) and it was found that the recycled fraction is slightly larger at

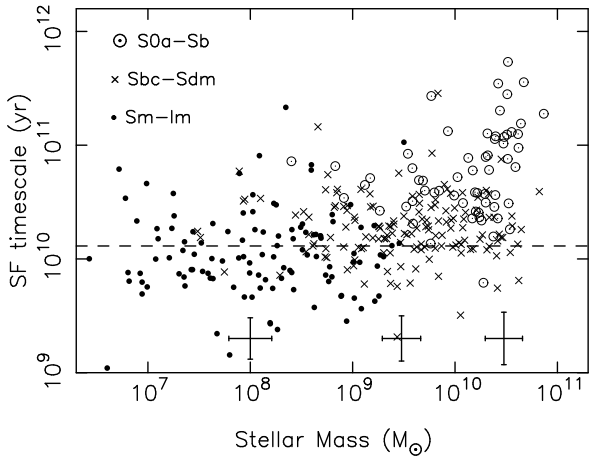

Fig. 2. The SF timescale as a function of galaxy stellar mass. The dashed line indicates the age of the Universe, 13.7 Gyr. Representative error bars are shown for the same three mass ranges as Fig. 1. In this case, the horizontal error bar includes an error due to galaxy distance uncertainties; the quantity plotted on the vertical axis is distance-independent.

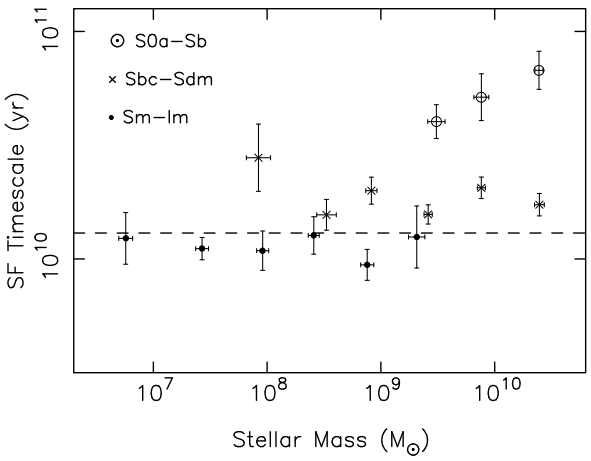

Fig. 3. Mean SF timescale as a function of galaxy stellar mass. The dashed line indicates the age of the Universe, 13.7 Gyr. Note the reduced vertical scale cf. Fig. 2.

low metallicity than at solar metallicity. However, the change in recycled fraction only leads to a 3.5% change in $(1-\mathcal{R})^{-1}$ for a 10 Gyr old population, for a change in [Fe/H] of +0.06 to –1.49. The change is smaller than this at younger ages (e.g. 2% at 1 Gyr).

Note that the recycling correction in Eq. (1) is appropriate because the calibrations of M/L by Bell & de Jong (2001) are in relation to remaining stellar mass, which is the more generally used definition of stellar mass, as opposed to the integral of the SF rate.

The SF timescale enables the identification of quiescent galaxies, for which this timescale will be much greater than a Hubble time, and galaxies currently in a starburst phase, for which it will be much less than a Hubble time.

Figure 2 shows the SF timescale values for individual galaxies in the HαGS sample, with stellar masses and internal extinction corrections derived from $M_{R,\mathrm{tot}}$ magnitudes, as explained in the previous section. The different point styles indicate galaxies in 3 different morphological type ranges: S0a – Sb, Sbc – Sdm, and Sm – Im. Representative error bars are shown for the same three mass ranges as Fig. 1. In this case, the horizontal error bar additionally includes an error due to galaxy distance uncertainties; the quantity plotted on the vertical axis is distance-independent. The distance errors, derived from a comparison of our values from James et al. (2004) with estimates in the literature, were taken as 20% in distance (44% in estimated luminosities and quantities derived from them) for galaxies nearer than 10 Mpc, which includes most of the Sm and Im types. For the more distant galaxies, the distance errors decrease to 10%.

Some trends and differences as a function of morphological type are already evident in Fig. 2, but are shown more clearly in Fig. 3, in which the individual galaxy SF timescales from Fig. 2 are binned over ranges of galaxy stellar mass. In Fig. 3, the quantity plotted for each type/mass bin is

$$\frac{\Sigma_i(\mathrm{mass}_i)}{\Sigma_i(\mathrm{SFR}_i)}\,\frac{1}{(1-\mathcal{R})} \qquad (2)$$

rather than the mean of the individual timescale values, to minimise the effect of outliers. Figure 3 shows clearly that the bulge-dominated early-type galaxies have high timescales, implying that their current SF rates are significantly lower than would be required to form the stellar mass within a Hubble time. The late-type Sm and Im galaxies, on the other hand, have uniformly short SF timescales, with binned means in the range 9–13 Gyr. Thus these bulge-free galaxies could have formed their stellar mass through continuous SF activity at or slightly below the current rate. It is important to note that the mass ranges of the different types overlap significantly, and the shorter SF timescales can be seen to depend only on the lack of a bulge, and not on galaxy mass. Another interesting feature of Fig. 2 is that the scatter in the late-type galaxy SF timescales is constant as a function of galaxy mass, at least over the range studied, and shows no sign of an increase at low galaxy masses and low SF rates, as would be expected if statistical fluctuations were dominating the scatter. This scatter will be analysed further in Sect. 5.

Star formation timescales of ~10 Gyr were also found for the field Magellanic irregulars studied by van Zee (2001), and for the dwarf irregulars in the M 81 group study of Karachentsev & Kaisin (2007); however, Skillman et al. (2003) found much longer timescales for dwarf irregular galaxies in the Sculptor group, which they identified as a possible transition dI – dE population. In all three studies, the methods employed were very similar to the present work. We also analysed SF rates and stellar masses from the Sloan Digital Sky Survey (SDSS) as derived by Brinchmann et al. (2004). Taking the Data Release Four sample, we selected galaxies with $0.008 < z < 0.1$, $17.5 < r < 17.75$ (near the limit of the main galaxy sample to minimise aperture effects) and an estimated SF rate. The data were then divided into low concentration, predominantly late types ($R50/R90 > 0.45$ in the r-band) and intermediate concentration ($0.35 < R50/R90 < 0.45$). Figure 4 shows a plot of the timescales in bins of 100 galaxies with the average as per Eq. (2) except a weight equal to $1/D^3$ was applied to each galaxy where D is the distance. This is because within a narrow magnitude range, the volume over which a galaxy could be observed is approximately proportional to D^3. The timescales are ~10 Gyr except at high masses where the contribution of earlier types comes in and at low masses where there are various complications with SDSS data such as incompleteness.

To conclude this section, we can propose a simple model of galaxy SF histories, consistent with the above findings. We find evidence of two modes of SF, one at a constant rate, and the

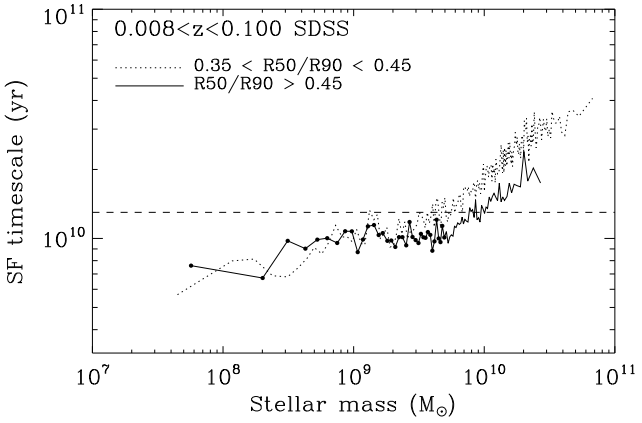

Fig. 4. Mean SF timescales derived from the SF rates and stellar masses of Brinchmann et al. (2004). The dashed line indicates the age of the Universe, 13.7 Gyr.

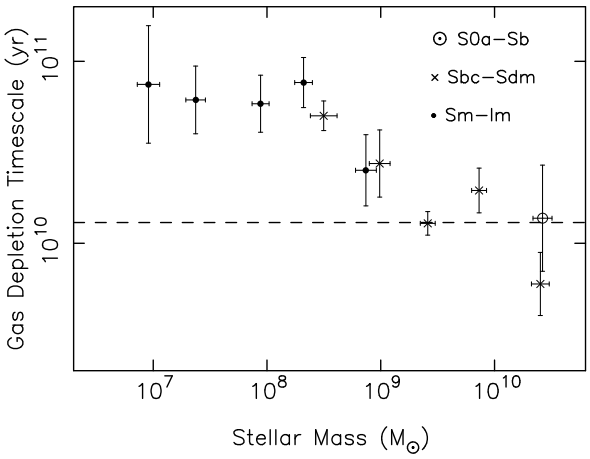

Fig. 5. Mean gas-depletion timescale plotted against galaxy stellar mass. The dashed line indicates the age of the Universe, 13.7 Gyr.

other dominated by an earlier burst. The Sm and Im late-type galaxies appear to be dominated by the first mode, whilst earlier type galaxies have a combination of the two modes, with the early burst becoming more dominant for earlier Hubble types and higher masses, at least within the earliest types.

4. Gas depletion timescales

Continued SF with no indication of a fall-off at the current epoch implies a substantial reservoir of gas in the galaxies concerned. This is confirmed in Fig. 5, which shows the gas depletion timescales for the 94 members of the current galaxy sample with HI masses provided by the Westerbork observations of neutral Hydrogen in Irregular and SPiral galaxies (WHISP) survey (Swaters et al. 2002). The HI masses are multiplied by 2.3 to account for helium and molecular gas; this factor was taken from Meurer et al. (2006) who base their calculation on H_2: HI ratios from the study of Young et al. (1996). The resulting gas mass divided by the SF rate, corrected as above for the recycling factor $\mathcal{R}$, gives the depletion time. In general, the HI is more widely distributed than the stellar component in galaxies; for example, Swaters et al. (2002) find the HI extents to be typically 1.8 those of the stars, with significant scatter. No correction was made for this effect, as even the outlying gas can be considered as ultimately available to fuel star formation.

Errors in gas masses were attributed to two causes: errors in the HI measurements from the WHISP study, and uncertainty in the conversion of HI to total gas masses. The former were taken from Swaters et al. (2002), who quote a 15% rms difference between their flux densities and those quoted in the literature for the same galaxies. They also comment that there should be no problems with large-scale flux being resolved out for galaxies as small as those studied here. Thus 15% was adopted as the error on HI flux density, and hence on atomic gas mass. The conversion constant of 2.3 is significantly more uncertain; for example, Garnett (2002) finds molecular gas fractions in many galaxies to be generally smaller than those found by Young et al. (1996). We adopt a 30% error from this cause, giving 34% overall errors in gas masses. These need to be added in quadrature to the SF rate errors, to give errors on the gas depletion timescales of 45–61%, the largest values being for the brightest galaxies.

Figure 5 shows that spiral galaxies can have short gas depletion times, particularly at high masses, in spite of their low specific SF rates implied by Figs. 2 and 3. The Sm/Im galaxies on the other hand have ample gas reservoirs to continue their current SF activity for much more than a further Hubble time. For those late-type galaxies with stellar masses below 10^9 $M_\odot$, there is a marked plateau in gas depletion times at 7×10^{10} years; these galaxies have sufficient fuel to continue their SF for several Hubble times, even without gas replenishment. Thus there is no contradiction or fine-tuning implied in the suggestion that the SF activity has continued unabated to the present epoch.

5. A determination of the "burstiness" of Sm/Im SF

We have argued in the previous sections that the properties of the late-type galaxies are consistent, on average, with their having assembled their stellar populations through SF at a constant rate that is similar to that currently observed. We now look in more detail to see to what extent this can be the case for individual galaxies.

A first point to note is that no completely passive Sm or Im galaxy is found in our sample of 117 objects. In every case, detectable Hα emission is found. This is significant, as the present sample is a substantial fraction of the total number of late-type dwarfs in the local Universe; we have observed 55% of the Sm and Im galaxies in the UGC that satisfy the HαGS selection criteria. Thus, unless we have been extremely unlucky in our selection, passive Sm and Im field galaxies must be extremely rare or non-existent. Such passive galaxies cannot be masquerading as dwarf ellipticals, as such objects are rare in the field environment. Some could evade detection by fading below selection limits, but this would require the passive phase to have continued for several Gyr to be a significant effect. Thus we conclude that all galaxies that have the gas reservoirs to support SF are in fact observed to form stars. This same conclusion was also reached by Meurer et al. (2006), who imaged 93 HI-selected galaxies in Hα and detected line emission in all of them. In addition, the analysis by Haines et al. (2007), using SDSS data, found all of the ~600 low-luminosity galaxies studied ($-18 < M_r < -16$) in the lowest-density environments to have Hα emission.

There is significant scatter in the SF timescales plotted in Fig. 2, which is consistent with SF rates in individual galaxies varying by factors of a few about the mean rate. Formally the scatter in SF timescale in Fig. 2 is 0.36 dex for types Sm and Im (cf. 0.26 dex for types Sbc to Sdm and 0.34 dex for types S0a

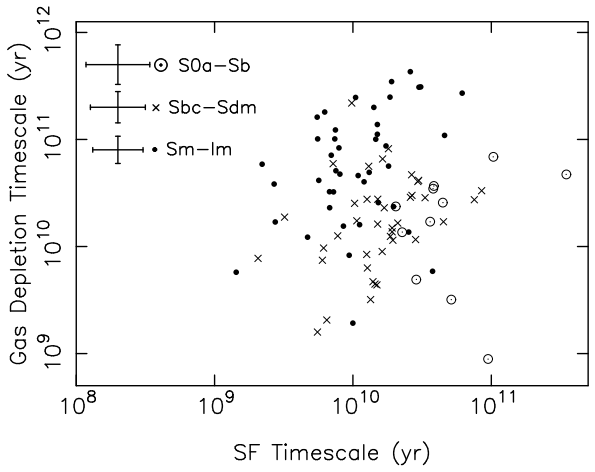

Fig. 6. Gas depletion timescale plotted against SF timescale, for the 94 galaxies with HI gas mass determinations. Representative error bars are shown for galaxies in each of the 3 T-type bins.

to Sb). From the error analysis presented earlier, the expected errors on SF timescale are 52% for the late-type galaxies, or 0.18 dex; thus, it would apear that the bulk of the vertical scatter in Fig. 2 is due to intrinsic variations in the SF timescale, and not just measurement error.

A further analysis of the burstiness of SF can be made using a technique similar to the one applied by Karachentsev & Kaisin (2007) to the study of galaxies in the M 81 group. In their Fig. 4, they plot a parameter $F_\star$, which is very similar to our SF timescale, against $P_\star$, which is closely related to our gas depletion timescale (with the main differences being that they normalise both parameters explicitly by the Hubble time, and $F_\star$ is based on B-band luminosity). They find a strong correlation between these parameters, which they interpret in terms of some galaxies being in starburst and quiescent phases, which respectively shorten and lengthen the timescales corresponding to these parameters. Figure 6 shows the equivalent plot for the 94 HαGS galaxies with HI gas mass determinations. Overall we find no correlation (correlation coefficient –0.02) between the SF and gas depletion timescales when considered across all galaxy types; however, for the 43 Sm and Im galaxies there is a marginally significant correlation at the 2.3 sigma level (correlation coefficient 0.33; significance 0.028) in the expected sense that galaxies with longer SF timescales also tend to have longer gas depletion timescales.

We can use Fig. 6 to quantify the burstiness of SF by noting that an instantaneous increase or decrease in SF rate will move points to the upper right or lower left, thus increasing the scatter along this 45° axis relative to that along the perpendicular axis. The additional scatter along this axis, that is required to explain the 2.3σ correlation implies a variation in SF rate by 0.247 dex, or a factor of 1.8 about the mean rate, for the Sm and Im galaxies. This modulation for our field sample is consistent with the scatter in both the SF and gas depletion timescales, which cannot be explained though measurement errors, and is substantially lower than that required to explain the findings of Karachentsev & Kaisin (2007) for the M 81 group. The stronger variation in SF rates that they find may be due partly to the M 81 group environment being ideally suited to strong inter-galaxy tidal interactions, and partly due to their sample including more very low luminosity galaxies where the intrinsic variations in SF rate may be more marked. Noeske et al. (2007), in a study of the long-term SF trends in field galaxies, find a gradually declining SF rate, with strong SF bursts being uncommon in their sample of galaxies, in good overall agreement with our findings.

Table 2. Modelled and observed stellar population colours.

Colour	[Fe/H] = –0.96	[Fe/H] = –0.25	Observed
$R-K$	1.84	2.09	1.865 ± 0.103
$J-K$	0.76	0.86	0.777 ± 0.018

6. Other tests of continuous SF histories in field late-type dwarfs

In this section we perform two final tests of the consistency of constant SF rates in Sm/Im galaxies with the observed galaxy properties. The first test addresses potential concerns over the use of the Bell & de Jong (2001) calibration of the mean stellar M/L ratios based on mean colours taken from the literature. This method raises several questions: do the mean properties apply to the specific galaxies observed here, how sensitive are the mass predictions to the particular stellar synthesis models used by Bell & de Jong, and does our proposed SF history result in a population with a M/L ratio consistent with that assumed in our calculation? In order to give complete independence from the Bell & de Jong models, we use use the BaSTI population synthesis code (Pietrinferni et al. 2004) for this test. This code was used to generate stellar populations with constant SF rates over a Hubble time and a range of stellar metallicities, and the resulting colours and M/L ratios were compared with those observed for galaxies in the present sample.

Photometry in the R band was taken from the HαGS database, and J and K total magnitudes were derived from the 2-Micron All-Sky Survey (Jarrett et al. 2003) as explained in Sect. 2. The mean $(R-K)$ and $(J-K)$ colours for the 21 Sm and Im galaxies from the present sample with available 2MASS data are listed in the final column of Table 2. The BaSTI model colours for stellar metallicities of [Fe/H] = –0.96 and –0.25 are listed in the second and third columns respectively.

The observed mean colours appear to agree best with those for a model [Fe/H] slightly higher than –0.96, i.e. similar to that generally found for the Small Magellanic Cloud ([Fe/H] ≃ –0.7). The M/L ratio of this same population is almost identical to that inferred earlier using the model of Bell & de Jong (2001), hence there is no inconsistency in using the mass from the latter model in calculating the SF timescale in Sect. 3.

We can also test whether the spatial distribution of newly-formed and old stellar populations is consistent in these galaxies. Figure 7 shows the normalised distributions of the mean R-band (dashed) and Hα (solid line) fluxes of all Sm (a) and Im (b) galaxies in the current sample. The vertical scale is flux within circular annuli (*not* surface brightness), normalised such that the total area under the curve, which represents the total flux, is unity for each galaxy. The horizontal scale is annular radius in units of the diameter of the galaxy at an R-band surface brightness of 24 mag/sq. arcsec. Thus this is a dimensionless shape function describing the averaged light distributions of all the Im galaxies, with all galaxies, large and small, receiving equal weight. Given the small number of HII regions in many of these galaxies, the individual galaxy Hα profiles are very spiky. In the mean, however, they look similar to the mean R-band light distribution, as is reflected by the small size of the residuals between the 2 profiles, in the sense $(H\alpha - R)$, shown by the dotted line in Fig. 7. If we take the R-band light to be a fair tracer of the distribution of the old stellar population, this is consistent

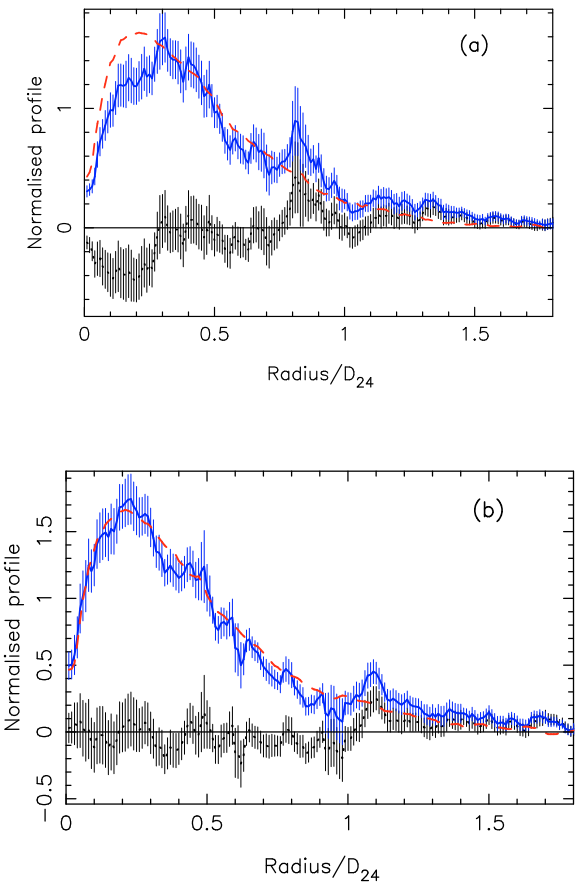

Fig. 7. a) Mean, normalized radial distributions of Hα (solid line) and R-band (dashed line) light for 42 Sm galaxies; the dotted line shows the residuals between these two profiles. **b)** The same mean profiles for the 75 Im galaxies.

with the overall stellar population having been produced by SF activity distributed like that observed at present.

7. Summary

We have studied the SF histories of 117 late-type Sm and Im field galaxies from the HαGS sample, using the variations in current properties to constrain the likely SF histories of galaxies of these types. The main conclusions are as follows:

- When averaged across the whole sample, the total stellar mass in these galaxies could have been formed by the extrapolation of the current SF rate over a Hubble time. This conclusion applies to Sm and Im galaxies across the full mass range studied, $10^7 - 10^{9.5}$ $M_\odot$. This confirms the conclusions of e.g. Hunter & Gallagher (1985) and van Zee (2001), but for a larger and more nearly complete sample.
- Disk galaxies of types S0a – Sb, and Sbc – Sdm, have current SF rates too low to accumulate their total stellar masses over a Hubble time, with the deficiency being most marked for the earliest types and largest masses. There is substantial overlap in the stellar mass ranges of these earlier types with the Sm/Im galaxies, so it appears to be the presence or absence of a bulge component that determines whether the mean SF timescale is greater than or equal to a Hubble time.
- Gas depletion timescales for the late-type galaxies are long compared with a Hubble time, and longer than those of earlier type galaxies.
- No completely quiescent Sm or Im galaxies are found in our sample; such galaxies must be very rare in the field population generally.
- An analysis of the correlation in the scatter of SF and gas depletion times implies a typical variation in the SF rate of a factor of 1.8 about the mean value.
- Population synthesis modelling assuming a constant SF rate accurately reproduces the mean colours and stellar M/L ratios found for the Sm and Im galaxies in the present sample.
- The mean spatial distribution of SF in the Sm and Im galaxies is consistent with the distribution of the old stellar population as seen in the R-band light.

Acknowledgements. M.P. acknowledges STFC for a postgraduate studentship. The Jacobus Kapteyn Telescope was operated on the island of La Palma by the Isaac Newton Group in the Spanish Observatorio del Roque de los Muchachos of the Instituto de Astrofísica de Canarias. This research has made use of the NASA/IPAC Extragalactic Database (NED) which is operated by the Jet Propulsion Laboratory, California Institute of Technology, under contract with the National Aeronautics and Space Administration. The referee is thanked for many helpful suggestions, which improved the content, clarity and presentation of the paper.

References

Almoznino, E., & Brosch, N. 1998, MNRAS, 298, 931
Barazza, F. D., Jogee, S., Rix, H.-W., et al. 2006, ApJ, 643, 162
Bell, E. F., & de Jong, R. S. 2000, MNRAS, 312, 497
Bell, E. F., & de Jong, R. S. 2001, ApJ, 550, 212
Brinchmann, J., Charlot, S., White, S. D. M., et al. 2004, MNRAS, 351, 1151
Chabrier, G. 2003, PASP, 115, 763
Dekel, A., & Silk, J. 1986, ApJ, 303, 39
Dekel, A., & Woo, J. 2003, MNRAS, 344, 1131
Gallagher, III, J. S., Hunter, D. A., & Tutukov, A. V. 1984, ApJ, 284, 544
Garnett, D. R. 2002, ApJ, 581, 1019
Gerola, H., Seiden, P. E., & Schulman, L. S. 1980, ApJ, 242, 517
Grebel, E. K., & Gallagher, III, J. S. 2004, ApJ, 610, L89
Haines, C. P., Gargiulo, A., La Barbera, F., et al. 2007, MNRAS, 381, 7
Helmboldt, J. F., Walterbos, R. A. M., Bothun, G. D., O'Neil, K., & de Blok, W. J. G. 2004, ApJ, 613, 914
Hoversten, E. A., & Glazebrook, K. 2007, ApJ, in press [arXiv:0711.1309]
Hunter, D. A., & Gallagher, III, J. S. 1985, ApJS, 58, 533
James, P. A., Shane, N. S., Beckman, J. E., et al. 2004, A&A, 414, 23
James, P. A., Shane, N. S., Knapen, J. H., Etherton, J., & Percival, S. M. 2005, A&A, 429, 851
Jarrett, T. H., Chester, T., Cutri, R., Schneider, S. E., & Huchra, J. P. 2003, AJ, 125, 525
Karachentsev, I. D., & Kaisin, S. S. 2007, AJ, 133, 1883
Kennicutt, Jr., R. C. 1983, ApJ, 272, 54
Kennicutt, R. C. 1998, ARA&A, 36, 189
Kennicutt, R., Tamblyn, P., & Congdon, C. 1994, ApJ, 435, 22
Kroupa, P. 2001, MNRAS, 322, 231
Lanfranchi, G. A., & Matteucci, F. 2003, MNRAS, 345, 71
Mayer, L., Governato, F., Colpi, M., et al. 2001, ApJ, 559, 754
Meurer, G. R., Hanish, D. J., Ferguson, H. C., et al. 2006, ApJS, 165, 307
Nilson, P. 1973, Uppsala general catalogue of galaxies (Acta Universitatis Upsaliensis, Nova Acta Regiae Societatis Scientiarum Upsaliensis – Uppsala Astronomiska Observatoriums Annaler, Uppsala: Astronomiska Observatorium, 1973)
Noeske, K. G., Weiner, B. J., Faber, S. M., et al. 2007, ApJ, 660, L43
Pietrinferni, A., Cassisi, S., Salaris, M., & Castelli, F. 2004, ApJ, 612, 168
Recchi, S., Hensler, G., Angeretti, L., & Matteucci, F. 2006, A&A, 445, 875
Salpeter, E. E. 1955, ApJ, 121, 161
Schlegel, D. J., Finkbeiner, D. P., & Davis, M. 1998, ApJ, 500, 525
Skillman, E. D., Côté, S., & Miller, B. W. 2003, AJ, 125, 593
Somerville, R. S. 2002, ApJ, 572, L23
Stinson, G., Seth, A., Katz, N., et al. 2006, MNRAS, 373, 1074
Stinson, G. S., Dalcanton, J. J., Quinn, T., Kaufmann, T., & Wadsley, J. 2007, ApJ, 667, 170
Swaters, R. A., van Albada, T. S., van der Hulst, J. M., & Sancisi, R. 2002, A&A, 390, 829
van Zee, L. 2001, AJ, 121, 2003
Weilbacher, P. M., & Fritze-v. Alvensleben, U. 2001, A&A, 373, L9
Young, J. S., Allen, L., Kenney, J. D. P., Lesser, A., & Rownd, B. 1996, AJ, 112, 1903